Journal of Thermal Analysis and Calorimetry, Vol. 95 (2009) 3, 713–719

THERMAL TRANSITIONS OF ACTIN

D. Lőrinczy[1*], *Zsuzsanna Vértes*[2], *Franciska Könczöl*[3] *and J. Belágyi*[1]

[1]Institute of Biophysics, University Pécs, Faculty of Medicine, Szigeti u. 12, 7624 Pécs, Hungary
[2]Institute of Physiology, University Pécs, Faculty of Medicine, Szigeti u. 12, 7624 Pécs, Hungary
[3]Institute of Forensic Medicine, University Pécs, Faculty of Medicine, Szigeti u. 12, 7624 Pécs, Hungary

Actin is one of the main components in the eukaryote cells which plays significant role in many cellular processes, like force-generation, maintenance of the shape of cells, cell-division cycle and transport processes.

In this study the thermal transitions of monomer and polymerized actins were studied to get information about the changes induced by polymerization and binding of myosin to actin using DSC and EPR techniques. The main thermal transition of F-actin was at 67.5°C by EPR using spin-labeled actin (the relative viscosity change was around 62°C), while the DSC denaturation T_ms were at 60.3°C for G-actin and at 70.5°C for F-actin.

Applying the Lumry–Eyring model to obtain the parameters of the kinetic process and calculate the activation energy, a 'break' was found for F-actin in the function of first-order kinetic constant *vs.* $1/T$. This indicates that an altered interdomain interaction is present in F-actin. The addition of myosin or heavy meromyosin (HMM) in different molar ratio of myosin to actin has changed significantly the EPR spectrum of spin-labeled F-actin, indicating the presence of the supramolecular complex. Analyzing the DSC traces of the actomyosin complex it was possible to identify the different structural domains of myosin and actin.

Keywords: *DSC, EPR, F-actin, G-actin, myosin, thermal unfolding*

Introduction

During muscle contraction the force development arises from the direct interaction of the two main components of the muscle, myosin and actin. The process is driven and governed by the energy liberated from the hydrolysis of ATP. The energy released from hydrolysis produces conformational changes in myosin and actin, which is manifested as an internal motion of myosin head while bound to actin [1–9]. The myosin heads attached to actin undergo to conformational changes during the hydrolysis process of ATP, which results in a strain in the head portion of myosin in an ATP-product dependent manner. These structural changes lead to a large rotation of myosin neck region relieving the strain.

Actin has a central role in muscle activity as an essential component of cytoskeleton and a partner of all myosin based motor system [10–16]. The actin based systems regulated through a lot of factor. Actin can exist in two forms: as a globular monomer, called G-actin, and after polymerization as a homopolymer, called filamentous or F-actin. During the polymerization process an ATP hydrolyses to ADP·P_i. According to [17] there are two F·ADP·P_i actin complexes according to the Scheme 1:

$$F\cdot ATP \Leftrightarrow F^*\cdot ADP.P_i \Leftrightarrow F\cdot ADP\cdot P_i \Leftrightarrow F\cdot ADP + P_i$$

(Scheme 1)

where F*·ADP·P_i complex is a product of ATP hydrolysis accompanying the actin polymerization and the inorganic phosphate P_i dissociates slowly from this complex.

In this work we tried to approach the temperature-induced unfolding processes in different actins prepared from striated muscle of rabbit. We have extended the experiments to study the interaction of F-actin with myosin and heavy meromyosin (HMM) prepared from psoas muscle of rabbit. In this work differential scanning calorimetry (DSC) was used, which is a sensitive and informative method for investigating the basic thermodynamic properties of proteins [18] giving information about their global states and domain interactions, and electron paramagnetic resonance spectroscopy (EPR) to look into the molecular dynamic processes. It was shown that by applying the Lumry–Eyring model [19, 20] for the determination of kinetic parameters of the thermal transitions, that the function of the first-order kinetic constant *vs*. reciprocal absolute temperature depends on the interaction between the domains forming the G-actin molecules. This supports the view that interdomain interactions determine the thermal behavior of actin in its different conformations.

* Author for correspondence: denes.lorinczy@aok.pte.hu

1388–6150/$20.00

Akadémiai Kiadó, Budapest, Hungary
Springer, Dordrecht, The Netherlands

The addition of myosin or HMM in different molar ratio of myosin to actin has changed significantly the EPR spectrum of spin-labeled F-actin, indicating the presence of a supramolecular complex. In the actomyosin complex after the denaturation the different structural domains of myosin and actin were quite clear separable.

Experimental

Materials and methods

Chemicals

Adenosine 5'-triphosphate (ATP), ADP, potassium chloride (KCl), magnesium chloride ($MgCl_2$), ethylene glycol-*bis*(β-aminoethyl ether)-N,N'-tetraacetic acid (EGTA), glycerol, 4-morpholinepropanesulfonic acid (MOPS), 4-maleimido-2,2,6,6-tetramethylpiperidinooxyl (MSL), phosphoenol pyruvic acid, pyruvate kinase were obtained from Sigma (Germany).

Actin preparation

Rabbit skeletal actin and heavy meromyosin (HMM) were isolated from the hind leg and back muscle of domestic white rabbits by standard methods [21, 22]. Actin was extracted from aceton-dried muscle powder at 0° C with 0.2 mM ATP, 0.1 mM $CaCl_2$ and 2 mM Tris·HCl buffer at pH 8.3 for 20 min. The extraction was followed by two polymerization-depolymerization cycles in the presence of 100 mM KCl and 0.5 mM $MgCl_2$ to remove the rest of the regulatory proteins. The concentration of actin was determined by measuring the optical absorption using a Genesys 5 type spectrophotometer (A(280 nm)= 0.63 mg mL^{-1} cm^{-1}). G-actin was centrifuged with 100000xg before EPR measurements in order to remove contamination of F-actin. Actin was polymerized by the addition of 100 mM KCl and 5 mM $MgCl_2$ (final concentrations). The polymerization process lasted for 1 h at room temperature.

Myosin from leg and back muscle was prepared according to Margossian and Lowey [22]. Purified myosin was either directly used or stored in 50% glycerol at –20°C. Heavy meromyosin was prepared by chymotryptic digestion of myosin according to Weeds and Pope [23] and was stored in the form of ammonium sulphate precipitate. Before use, ammonium sulphate was removed by exhaustive dialysis against actin buffer solution with omission of ATP. The dialysis was followed by 1 h centrifugation at 100000xg.

DSC technique

The thermal unfolding of actin and actomyosin proteins was monitored by a Setaram Micro DSC-II calorimeter. All experiments were done between 5 and 80°C. The heating rate was 0.3 K min^{-1}. Conventional Hastelloy batch vessels were used during the denaturation experiments with 850 μL sample volume in average. Preparation buffers were used as reference samples. The sample and reference vessels were equilibrated with a precision of ±0.1 mg. There was no need to do any correction from the point of view of heat capacity between the sample and reference vessels. The samples were irreversible denatured during each cycle. The repeated scan of denatured sample was used as baseline reference, which was subtracted from the original DSC curve. Calorimetric enthalpy was calculated from the area under the heat absorption curve using two-point setting Setaram peak integration. The DSC diagrams were deconvolved by the PeakFit 4.12 program from SPSS Corporation after data correction. In order to describe the single transitions Gaussian or exponentially modified Gaussian (EMG) functions were used.

Spin-labelling

Spin-labelling of actin with MSL was performed in F-form with 1.2 molar excess of label to mole of protein for 2 h at 0°C. The labelled F-actin was pelleted by 40000 rpm, then the pellet was homogenised and dialysed overnight in G-buffer (4 mM Tris-HCl, pH 7.6, 0.2 mM ATP, 0.2 mM $CaCl_2$).

EPR measurements

Conventional EPR spectra were taken with an ESP 300E (Bruker Biospin, Germany) X-band spectrometer. First harmonic, in-phase, absorption spectra were obtained using 20 mW microwave power and 100 kHz field modulation with amplitude of 0.1 or 0.2 mT at different temperature from 0 to 70°C. For all spectra, sweep width was 10 mT, sweep time 81 s, time constant 20.4 ms, conversion time 41 ms and 10 scans were accumulated. The samples were placed in a flat quartz cell (Scanlon Co., USA, capacity about 80 μL), and spectra were recorded immediately after mixing the components. Second harmonic, 90° out-of-phase absorption spectra were recorded with 63 mW and 50 kHz field modulation of 0.5 mT amplitude detecting the signals at 100 kHz out-of-phase. The 63 mW microwave power corresponds in average microwave field amplitude of 0.025 mT in the centre region of the cell, and the values were obtained by using the standard protocol of Fajer and Marsh and Squier and Thomas [24, 25]. The spectra were normalized to the same number of unpaired electrons calculating the double integrals of the derived spectra, and the manipulations were performed on normalized EPR spectra.

Results and discussion

In this study the thermal transitions of actin in monomer and as well as in polymerized forms were studied to get information about the changes induced by polymerization and binding of myosin to actin using DSC and EPR techniques. The main transition of G-actin (Fig. 1) was at 60.3°C by DSC, whereas 67.5°C was derived for F-actin (Fig. 2). Similarly, using the EPR technique, the spectra of Cys-374 labeled G-actin at about 60°C showed practically no immobilized fraction of reporter molecules which is the sign of a complete unfolding of the protein, at least in the environment of the labeled sites (Fig. 3). In the case of F-actin the unfolding was detected at significantly higher temperature at the vicinity of 70°C (Fig. 4). The transition temperature varied between 67.5 and 70°C, depending on preparation. In contrast to EPR and DSC measurements the abrupt change of relative viscosity of actin solution at increasing temperature was observed much lower temperature around 62°C (not shown).

It is well-known from structural studies that actin is a globular protein molecule; each actin monomer has two dissimilar globular parts, the large domain (subdomain 3 and 4) and the small domain (subdomain 1 and 2) connected by a narrow cleft. The stability of this connection is ensured by a divalent cation (usually Ca^{2+}-ion in standard biochemical preparations in G-form and Mg^{2+}-ion in F-form) and a nucleotide; in G-form usually ATP and after polymerization of G-actin the bound nucleotide is ADP. The nucleotide locates in the cleft between the domains, and at the bottom of the cleft is the divalent

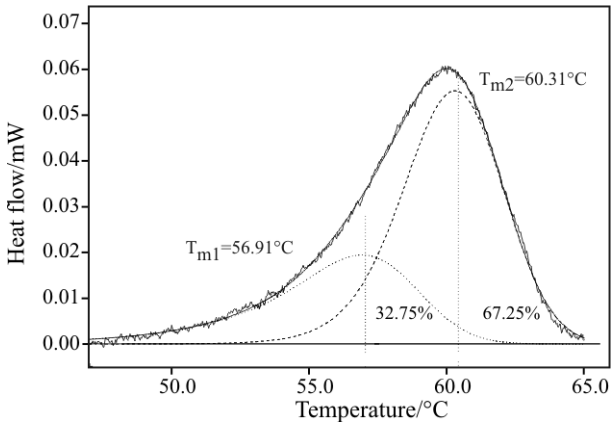

Fig. 1 DSC trace of G-actin as a function of heat flow (mW) *vs*. temperature (°C). Dotted and dashed lines show the deconvolved parts of the transition curve. Deconvolution was performed with exponentially modified Gaussian functions. It was suggested that the monomer actin has two main domains which behave as autonomic subunits

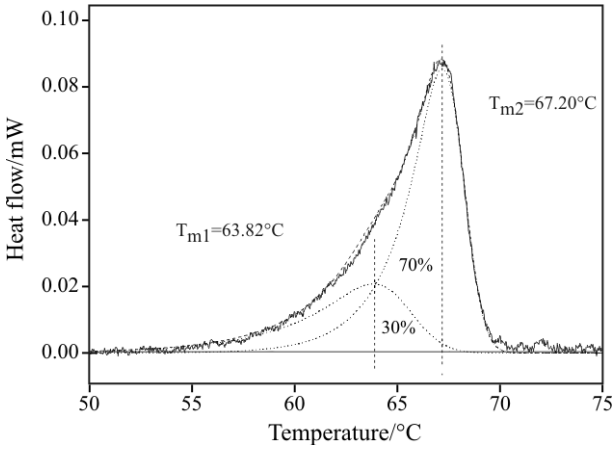

Fig. 2 DSC trace of polymerized actin. Note the higher temperatures of the transitions and the similar areas of the deconvolved parts of F-actin as observed in G-actin. Deconvolution was made with exponentially modified Gaussian functions

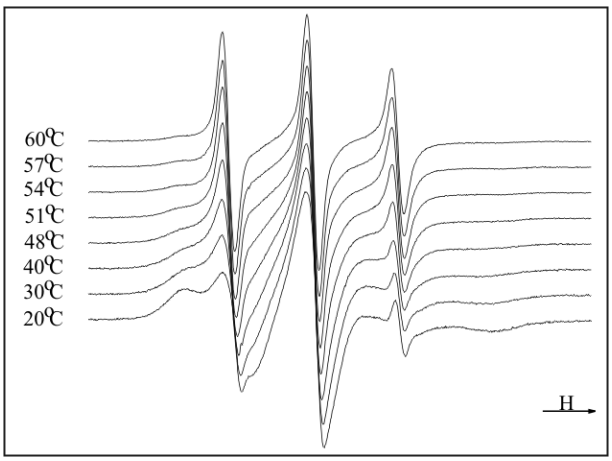

Fig. 3 EPR spectra of MSL-G-actin as a function of temperature. At about 60°C only the spectrum of the weakly immobilized probe molecules can be seen. The reporter molecules are attached to Cys-374 residue of G-actin. Note the larger components of the weakly immobilized probe molecules

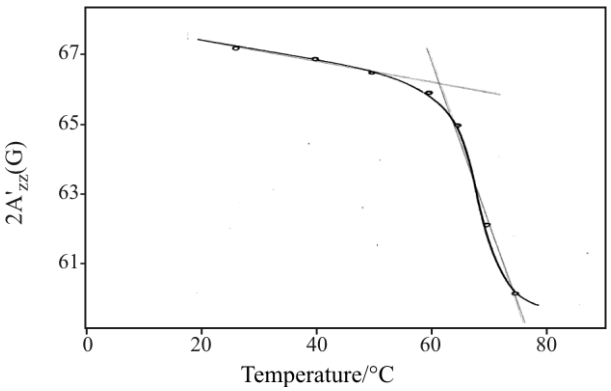

Fig. 4 Hyperfine splitting constant of the EPR spectra for MSL-F-actin as a function of temperature

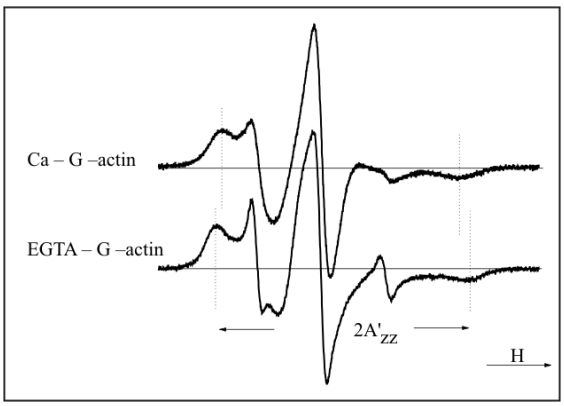

Fig. 5 EPR spectra of MSL-Ca-G-actin and EGTA-G-actin. Removing the Ca^{2+}-ions with EGTA the hyperfine splitting constant increased implying the change of the hydrodynamic radius of the actin monomers

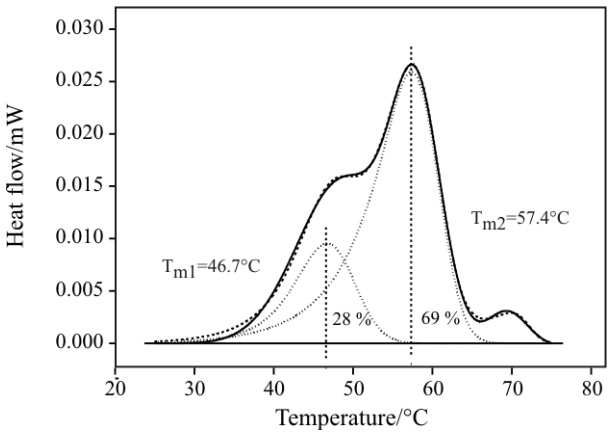

Fig. 6 DSC trace of EGTA-G-actin. Deconvolution with exponentially modified Gaussian functions resulted two transitions with lower transition temperatures in comparison with Ca-G-actin. Note the similar areas of the component transition curves in comparison with Ca-G-actin. Dashed line shows the sum of the deconvolved curves

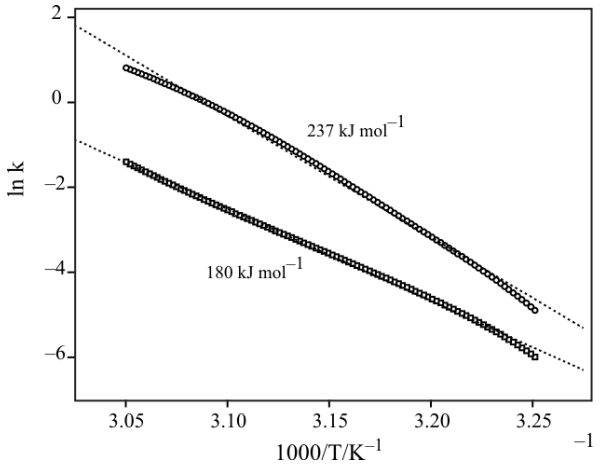

Fig. 7 Plot of ln*k* as a function of temperature for EGTA-G-actin. The larger activation energy belongs to the domain with higher transition temperature

metal ion. The two domains can rotate by 5° with respect to one another without change in the ATP binding site. The rotation allows a greater solvent accessibility of the nucleotide phosphate groups. Removing the divalent cation by 0.2 mM EGTA, the structure became instable measured by EPR (Fig. 5). The rotational correlation time increased from 13.6 to 42.5 ns, which is due to a large change of the hydrodynamic radius of the monomer [26]. The rotational correlation time of the more mobile component is about 1.3 ns. This value is not very far from the rotational correlation time of the free reporter molecule. It can be suggested that the quasi-independent motion of the two domains in the absence of divalent cation should have some consequences to the thermal denaturation process of the protein.

Figure 6 shows the DSC curve of EGTA-treated G-actin. The prominent two peaks appeared at 46.7 and 57.4°C clearly indicates the presence of two transitions. As consequences of the both EPR and DSC measurements we can suggest that the two domains in the absence of divalent cation behave as two quasi-independent domains. Deconvolution of the DSC trace by exponentially modified Gaussian functions resulted in two transitions with contributions of 29 and 70% of the heat absorption. Using the Lumry–Eyring model for the determination of the activation energies of the deconvolved thermal transitions we calculated 180 and 237 kJ mol^{-1}, respectively (Fig. 7). Similar calculation for Ca-G-actin resulted in 344 kJ mol^{-1} for the activation energy, and the natural logarithm of the reaction rate constant (k) as a function of $1/T$ was linear. The bound divalent cation in Ca-G-actin modifies the internal dynamics of the monomer actin; it decreases the flexibility and increases mobility within the whole molecule and profoundly affects the cooperativity between the domains. From the experiments we cannot conclude whether the unfolding of the domains occurs according to independent transitions or sequential transitions, and how large is the remaining interaction between the domains when one of the domains – very likely the small domain – is already in unfolded state in the absence of Ca^{2+}-ion. When we accept the existence of two structural domains in Ca-G-actin from the point of view of the thermodynamic behavior, then it is possible to perform the deconvolution on the DSC trace of Ca-G-actin (Fig. 1). The calculation gave upward shifts in the transition temperatures, 55.6 and 60.3°C, respectively. The calculated differences can be accounted for the interdomain interaction.

Analysis of the thermal transition of F-actin with the above mentioned model led to the observation that the plot of the natural logarithm of the reaction rate constant *vs*. reciprocal absolute temperature in not ex-

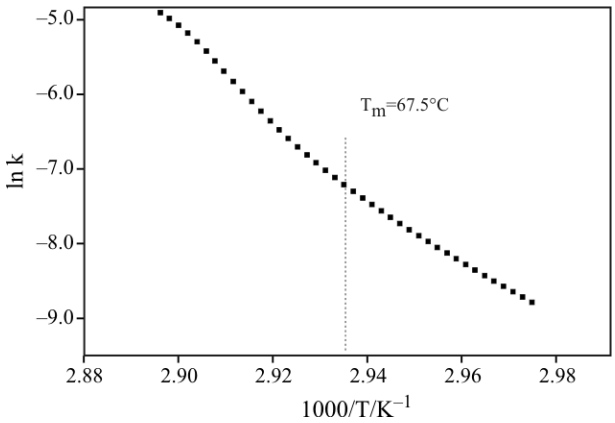

Fig. 8 Plot of ln*k* as a function of temperature for F-actin. At higher temperatures significant deviation can be obtained from the linear approximation

actly linear (Fig. 8). It suggests a strong cooperative interaction not only between the domains of the protomers, but it is necessary to take into account the intrastrand and interstrand interaction of the protomers. These interactions lead to the narrow width of the DSC trace, and might affect the activation energy during the unfolding process. Deconvolution with exponentially modified Gaussian function resulted in two transitions (Fig. 2). It is an interesting observation that the deconvolved areas of the transition curves are comparable in all three cases: Ca-G-actin, EGTA-G-actin and F-actin.

Myosin the main component of muscle tissue is a multidomain protein consisting of two identical heavy chains and two pairs of light chains; the globular heads are joined to a long rod. The long rod is formed from a two-stranded α-helical coiled coil. Figure 9 shows the DSC diagram of myosin solution. It was possible to identify tree transitions by deconvolution using Gaussian functions at 44.3, 51.1 and 59.9°C. These values agree quite well with the values

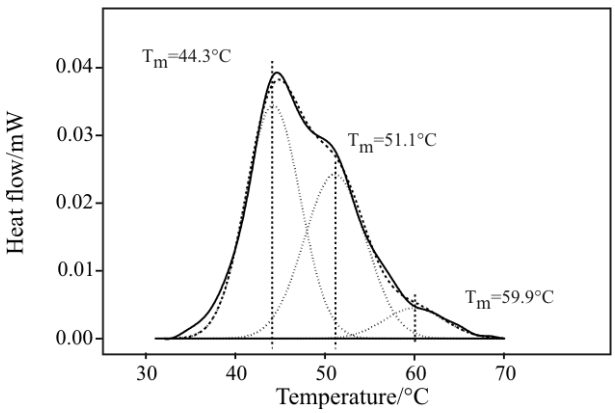

Fig. 9 DSC curve of myosin solution. It was possible to decompose the trace into three Gaussian transitions which corresponds to the multi-domain structure of myosin. Dashed line shows the sum of the deconvolved transitions

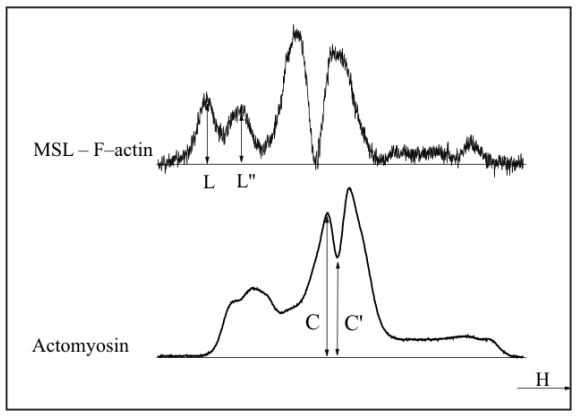

Fig. 10 Saturation transfer EPR spectra of MSL-F-actin and its complex with myosin. The large change of L''/L spectral parameter shows the increased rotational correlation time of the bound reporter molecules. Molar ratio of myosin to actin was 0.25 M myosin to 1 M of actin

of earlier observations [27, 28]. The two larger transitions can be assigned to the globular heads and the rod. Addition of F-actin to myosin results in a complex protein called actomyosin. Saturation transfer EPR spectra of MSL-F-actin and MSL-F-actin in combination with myosin (molar ratio of myosin to actin was 0.25 to 1) are shown in Fig. 10. The characteristic parameters L''/L and C'/C changed significantly after addition of myosin to actin which means that the rotational correlation time of the label on F-actin increased. In order to have an indication about the change of rotational motion after binding of myosin to F-actin, the nomograms published by Thomas and co-workers for Brownian rotational diffusion were used [29]. The estimated effective rotational correlation time increased from L''/L=100 to 800–1000 μs, and from C'/C=7 to 100 μs in actomyosin complex.

The DSC trace of the protein complex is shown in Fig. 11. Using Gaussian functions for decon-

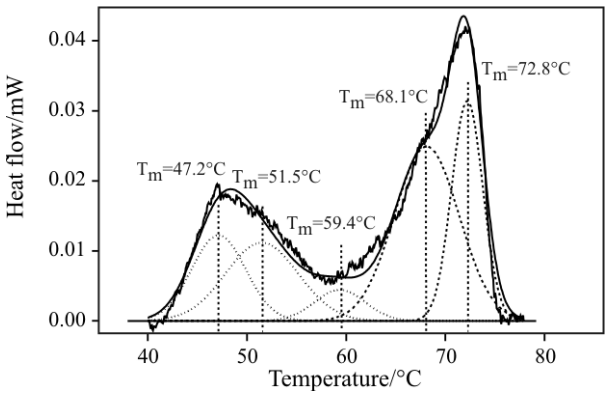

Fig. 11 DSC trace of actomyosin complex. Deconvolution was performed with Gaussian functions and resulted in five subunits. Dashed line indicates the sum of component transitions

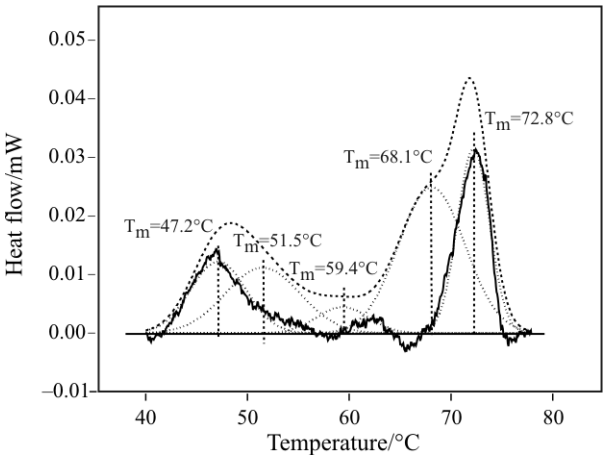

Fig. 12 Computer manipulation of the DSC trace for actomyosin. The components responsible for the myosin rod and for the smaller domain of F-actin were subtracted from the original DSC curve in order to obtain the components which account for the interaction between myosin and F-actin. Dashed line shows the original DSC trace of actomyosin

volution it was possible to resolve the contributions of different domains in the complex DSC curve (dotted lines in Fig. 12). From the comparison of the DSC trace of the actomyosin complex with that of the composite molecules we can conclude that two domains contribute significantly to the altered DSC curve. The structural model of actomyosin complex obtained by docking the atomic structure of head to the model of F-actin showed that the head can bind to several sites on actin [30–32]. The globular heads attach to the domains of F-actin and the binding induce an increased mutual internal stability in both domains; after computer manipulation we could conclude about 3°C upward shifts appear during the unfolding of myosin heads and about 2°C increase in one of the domains of F-actin (Fig. 12). This change also indicates that the environment of the labelled site is involved in the interaction of the two proteins. Fluorescence measurements on F-actin reported that subdomain 2 also participates in the interaction with myosin [33].

Conclusions

Our results support the well known fact that actin is a really 'active' partner in the muscle contraction. The thermal analytical method is a suitable one to follow its possible conformational changes during denaturation both in G as well as in F-actin forms. We have obtained valuable informations for the possible conformational changes during the interaction between myosin and actin in actomyosin complex, and for its energetical consequences too. These data are in good agreement with former results [34].

Acknowledgements

The Setaram Micro DSC-II was purchased with a grant (CO-272) from the Hungarian Scientific Research Fund (D. Lőrinczy). ESP 300E EPR spectrometer was purchased with a grant (CO-123) from the Hungarian Scientific Research Fund (Joseph Belágyi).

References

1 M. A. Geeves, Biochem. J., 274 (1990) 1.
2 K. C. Holmes, Acta Cryst., A54 (1998) 789.
3 K. C. Holmes, Nature Struct. Biol., 5 (1998) 940.
4 M. A. Geeves and K. C. Holmes, Ann. Rev. Biochem., 68 (1999) 687.
5 I. Rayment, H. M. Holden, M. Whittaker, C. B. Yohn, M. Lorenz, K. C. Holmes and R. A. Milligan, Science, 261 (1993) 58.
6 R. Dominguez, Y. Freyzon, K. M. Trybus and C. Cohen, Cell, 94 (1998) 659.
7 A. J. Fisher, C. A. Smith, J. Thoden, R. Smith, K. Sutoh, H. M. Holden and I. Rayment, Biophys. J., 68 (1995) 19s.
8 A. J. Fisher, C. A. Smith, J. Thoden, R. Smith, K. Sutoh, H. M. Holden and I. Rayment, Biochemistry, 34 (1995) 8960.
9 E. Pate, N. Naber, M. Matuska, K. Franks-Skiba and R. Cooke, Biochemistry, 36 (1997) 12155.
10 H. H. Chowdhury, M. R. Popoff and R. Zorec, Pflügers Arch., 439 (2000) R148.
11 P. Cossart, Curr. Opin. Cell Biol., 7 (1995) 94.
12 N. Guillen, M. F. Carlier, G. Brugerolle, I. Tardieux and J. Ausseil, Parasite, 5 (1998) 107.
13 S. Rice, A. W. Lin, D. Safer, C. L. Hart, N. Naber, B. O. Carragher, S. M. Cain, E. Pechatnikova, E. M. Wilson-Kubalek, M. Whittaker, E. Pate, R. Cooke, E. W. Taylor, R. A. Milligan and R. D. Vale, Nature, 402 (1999) 778.
14 C. Lamaze, L. M. Fujimoto, H. L. Yin and S. L. Schmid, J. Biol. Chem., 272 (1997) 20332.
15 J. B. Marchand, P. Moreau, A. Paoletti, P. Cossart, M. F. Carlier and D. Pantaloni, J. Cell Biol., 130 (1995) 331.
16 T. D. Pollard, Curr. Biol., 5 (1995) 837.
17 C. Combeau and M. F. Carlier, J. Biol. Chem., 263 (1988) 17429.
18 J. E. Ladbury and I. M. Doyle, Biocalorimetry, John Wiley and Sons Ltd. (2004)
19 J. M. Sanchez-Ruiz, J. L. Lopez-Lacomba, M. Cortijo and P. L. Mateo, Biochemistry, 27 (1988)1648.
20 R. Lumry and H. Eyring, J. Phys. Chem., 58 (1954) 110.
21 J. A.Spudich and S. Watt, J. Biol. Chem., 246 (1971) 4866.
22 S. S. Margossian and S. Lowey, Methods Enzymol., 85 (1982) 55
23 A. G. Weeds and B. Pope, J. Mol. Biol., 111, 129.
24 P. G. Fajer and D. Marsh, J. Magn. Res., 49 (1982) 212.
25 T. C. Squier and D. D. Thomas, Biophys. J., 49 (1986) 921.

26 M. Mossakowska, J. Belágyi and H. Strzelecka-Golaszewska, Eur. J. Biochem., 175 (1988) 557.
27 D. Lőrinczy, F. Könczöl, L. Farkas, J. Belágyi and C. Schick, J. Therm. Anal. Cal., 66 (2001) 633.
28 D. Lőrinczy, U. Hoffmann, L. Pótó, J. Belágyi and P. Laggner, Gen. Physiol. Biophys., 9 (1990) 589.
29 D. D. Thomas, L. R. Dalton and J. S. Hyde, J. Chem. Phys., 65 (1976) 3006.
30 I. Rayment, H. M. Holden, M. Whittaker, C. B. Yohn, M. Lorenz, K. C. Holmes and R. A. Milligan, Science, 261 (1993) 58.
31 I. Rayment, W. R. Rypniewski, K. Schmidt-Base, R. Smith, D. R. Tomchick, M. M. Benning, D. A. Winkelman, G. Wesenberg and H. M. Holden, Science, 261 (1993) 50.
32 K. C. Holmes, D. Popp, W. Gebhard and W. Kabsch, Nature, 347 (1990) 44.
33 E. Kim, C. J. Miller, M. Motoki, K. Seguro, A. Muhlrad and E. Reisler, Biophys. J., 70 (1996) 1439.
34 D. Lőrinczy and J. Belágyi, J. Therm. Anal. Cal., 90 (2007) 611.

DOI: 10.1007/s10973-008-9406-3